2021 IEEE/ASME International Conference on
Advanced Intelligent Mechatronics (AIM)

Calibration of tactile/force sensors for grasping with the PRISMA Hand II

D.E. Canbay [2], P. Ferrentino[1], H. Liu [1], R. Moccia [1], S. Pirozzi [3], B.Siciliano [1], F. Ficuciello [1]

***Abstract*—The PRISMA Hand II is a mechanically robust anthropomorphic hand developed at PRISMA Lab, University of Naples Federico II. The hand is highly underactuated, three motors drive 19 joints via elastic tendons. Thanks to its particular mechanical design, the hand can perform not only adaptive grasps but also in-hand manipulation. Each fingertip integrates a tactile/force sensor, based on optoelectronic technology, to provide tactile/force feedback during grasping and manipulation, particularly useful with deformable objects. The paper briefly describes the mechanical design and sensor technology of the hand and proposes a calibration procedure for tactile/force sensors. A comparison between different models of Neural Networks architectures, suitable for sensors calibration, is shown. Experimental tests are provided to choose the optimal tactile sensing suite. Finally, experiments for the regulation of the forces are made to show the effectiveness of calibrated sensors.**

***Index Terms*—robotic hand, force/tactile sensors, neural networks models, force regulation.**

I. Introduction

Substantial progress has been made in building anthropomorphic hands in the past two decades, using emerging technologies, both for robotic and prosthetic applications. Currently, there are several anthropomorphic hands available in the market, for example, the Bebionic Hand (Ottobock GmbH.), the i-Limb Hand (Touch Bionics Ltd.) and the Brunel Hand (Openbionics Ltd.).

Inspired by the human hand, compliance and sensors have been introduced to robotic hands, using different technological solutions, to improve robustness by absorbing external impact and capabilities in object grasping and manipulation. Elastic actuation has been introduced, by means of series elastic tendons [1], compliant links made from steel layers [2], and elastic joints, including flexure-based [3]–[5] and spring-based [6]. The PISA/IIT SoftHand [7] and the SoftHand Pro-H [8], using COmpliant Rolling-contact Elements (CORE) joint, are particularly interesting for our design. The DEXMART hand [9] is a good example of anthropomorphic solution with an advanced sensing system, evaluated for the development of PRISMA Hand II.

[1]P. Ferrentino, H. Liu, R. Moccia, F. Ficuciello, B. Siciliano, are with the Department of Information Technology and Electrical Engineering, Universitá degli Studi di Napoli Federico II, 80125 Napoli, Italy. [2]D.E. Canbay is with the Department of Mechatronics Engineering, Istanbul Technical University, Istanbul, Turkey. [3]S.Pirozzi is with Department of Engineering, Universitá degli Studi della Campania Luigi Vanvitelli. Corresponding author's email: salvatore.pirozzi@unicampania.it

This project has received funding from the European Union's Horizon 2020 research and innovation programme under grant agreement No.101017008, and from PNR 2015-2020 Italian National programme within PROSCAN project (CUP UNINA: E26C18000170005

While the grasping capability of robotic hands is steadily improving and approaching human performance [10]–[12], the remaining gaps with the human hand are related to dexterity, particularly in-hand manipulation dexterity, mostly in presence of deformable objects. The capability of in-hand manipulation brings better accuracy and efficiency to the upper-limb, as observed from the human [13], [14]. Recently developed fully-actuated hand, for example, the Shadow Dexterous Hand, the KITECH hand [15] and the BCL-13 [16], have demonstrated some level of in-hand manipulation dexterity, benefiting from independently driven finger joints. However, a fully-actuated hand is challenging in design, in particular, the major difficulty is to integrate a large number of actuators. It is also challenging in control for prosthetic applications, given the limited bandwidth of bio-signal interfaces that can be utilized for control.

For these reasons, researchers are moving their interests into designing underactuated hands, where the degrees of actuation (DoAs) is used to drive higher degrees of freedom (DOFs). Recently, a framework of performing efficient grasp [4], [7], [17]–[19] and in-hand manipulation by utilizing the elasticity of underactuated fingers, extended the functionality of underactuated hands [20]. Several robotic hands with in-hand manipulation capabilities have been introduced, e.g. iRobot-Harvard-Yale (iHY) hand [5], the GR2 gripper [21], [22], the caging manipulation gripper [23] and the Pisa/IIT SoftHand 2 [24]. Regarding tactile/force sensors, the main goal is to find low-cost technology that can be integrated in small spaces in order to improve the manipulation capabilities of the robotic hand. Very few commercial devices are currently available, even though many technologies have been proposed in the scientific literature to build tactile sensors like resistive, piezoelectric, capacitive, magnetic and optoelectronic [25]. The tactile/force sensor presented in this paper uses the technology proposed in [26], where the working principle has been presented for the first time and it exploits the studies based on Finite Element (FE) modeling conducted in [27]. In [26] for the first time also a neural network has been trained to evaluate the possibility to reconstruct force components from the tactile map. However, no comparison among different machine learning approaches, neither evaluations of the estimation quality were done.

In this paper, after a brief description of the PRISMA hand II and of the tactile sensors integrated into, a calibration solution for all tactile sensors available on the robotic hand is proposed. The solution compares different neural networks in

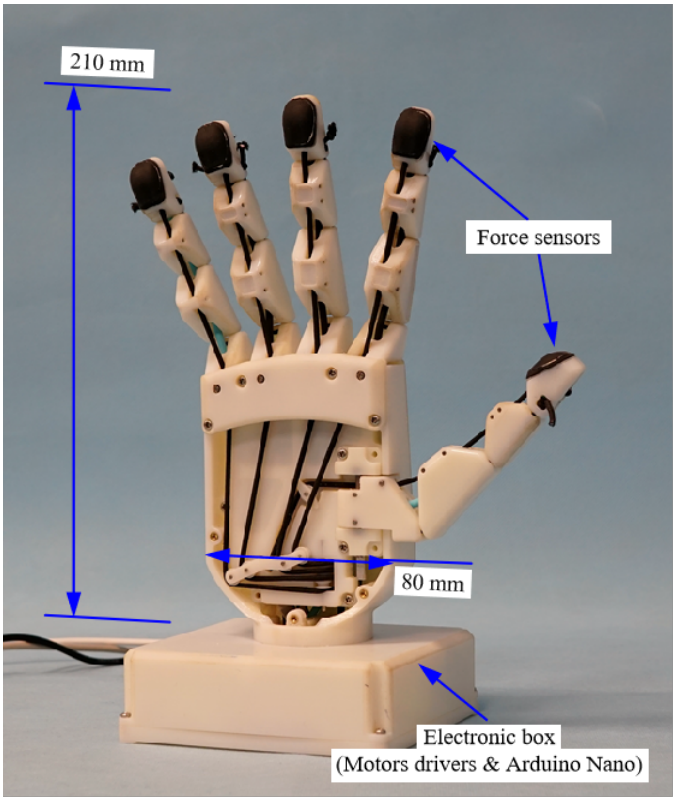

Fig. 1. The PRISMA Hand II

order to evaluate their effectiveness also trough experimental validation.

II. Brief description of the mechanical design

The PRISMA hand II (Fig. 1), presented for the first time in [28], has 19 joints and three motors (see Fig. 2(a)). Each finger is shown in Fig. 2(b) and has three flexion/extension joints consisting of compliant rolling joints. The thumb has one rotation joint, while the other fingers have one abduction/adduction joint, all consisting of revolute joints. The finger flexion joints adopt the rolling contact joint [29], which consists of a pair of surfaces in rolling contact with each other, with elastic elements holding them together. Each joint consists of a base link, a distal link, two ligaments, and a tendon. The ligaments, made of elastic string, are attached to the base link and the distal link. The tendon, which is made of the same elastic string, is anchored to the distal link and threaded through the hole of the base link. By pulling the tendon, the distal link is actuated and rolled on the cylindrical surface of the base link. Once the driving tendon is released, the elastic ligaments return the distal link to the extended position, similar to a torsional spring in a conventional pin joint. The elastic tendon and ligaments determine the joint multi-directional compliance, by allowing various disarticulation, including backward bend, sideway bend, twist, and dislocation. The video [1] shows additional features of the hand.

[1]https://www.youtube.com/watch?v=Rxg6iGle_6o

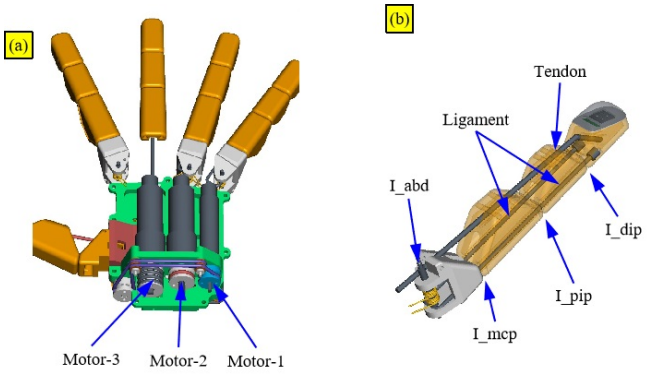

Fig. 2. Actuation strategy of PRISMA Hand II (a) and finger design (b).

III. The tactile/force sensor technology

The proposed tactile/force sensor has been suitably designed to be integrated into the PRISMA Hand II fingertip. Its dimensions are reported in Fig. 3(a). The design is based on the use of LED-phototransistor couples (corresponding to the sensible points), organized as a matrix on a Printed Circuit Board (PCB), and exploited to measure the deformation of an elastic layer positioned above the optoelectronic devices, as shown in Fig. 3(b). The obtained tactile map, after a calibration procedure, can be used to estimate the force applied to the deformable layer.

The PCB is constituted by four photoreflectors (code NJL5908AR, manufactured by New Japan Radio) organized as a 2×2 matrix, with a spatial resolution equal to 3.4 mm. Each photoreflector integrates, in the same package, an infrared Light Emitting Diode (LED) with a peak wavelength @ 920 nm and a Photo-Transistor (PT) with a peak wavelength @ 880 nm. The LED of each couple illuminates the reflective bottom surface of the deformable layer, while the phototransistor receives the reflected light and transduces it into a current. The deformable pad (see Fig. 3(c)) was cast by using silicone molding technology, and it is composed of a top layer of black silicone to avoid cross-talk problems between taxels and environment light disturbances and a bottom layer of white silicone to increase the sensor sensitivity, ensuring the maximum light reflection. The whole pad has been realized by using the MM928 silicone, manufactured by ACC Silicones, with a hardness equal to 26 Shore-A. This hardness is sufficiently low to allow the manipulation of deformable and fragile objects with a good sensitivity as shown in the following sections.

When an external force is applied, the deformable layer produces some local variations in the bottom surface of elastic material which induces a variation of the reflected light intensity and, consequently, a variation of the current flowing into the phototransistor. The relation between the emitted and the received light, with respect to the distance of the reflecting surface, is non-monotonic according to the datasheet of the photoreflectors. As the distance reduces, the received light goes up, by reaching the maximum value at

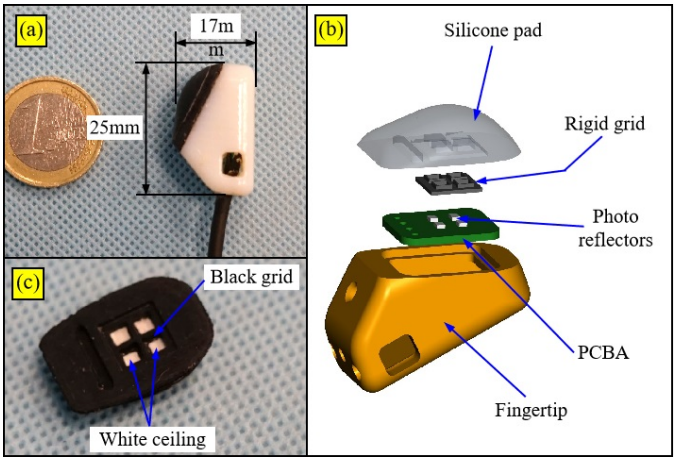

Fig. 3. PRISMA hand II fingertip assembly: fingertip dimensions (a), assembly of a tactile/force sensor (b) and silicone pad features (c).

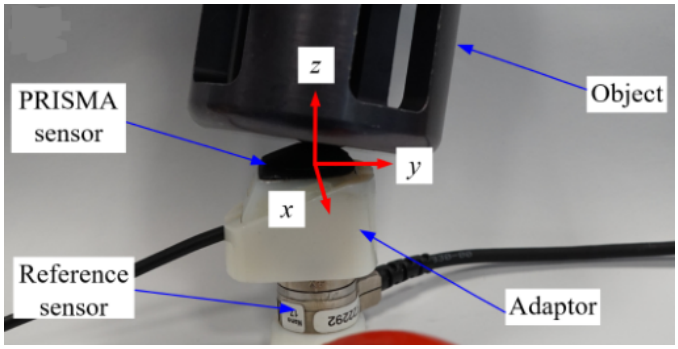

Fig. 4. Calibration setup.

0.25 mm distance of the reflecting surface. Then, if the distance further decreases, the received light drops. To avoid the non-monotonicity, a suitably designed rigid grid is introduced between the PCB and the silicone pad. The rigid grid has been printed with black plastic to reduce cross-talk among sensing points. Also the design of the curvature for the deformable pad has been defined in order to have a local curvature with a radius sufficiently small, to consider the contact surface with everyday objects always approximated as a contact with a flat surface.

Moreover, the maximum force level can be adapted by changing the hardness of the deformable layer. With the selected material the reachable force levels are equal to some newtons as presented in the calibration section, similarly to the human touch. The maximum measurable force is also limited by the maximum vertical deformation that each reflecting surface can reach. Also this last parameter can be optimized on the basis of final application.

IV. Sensor Calibration

Each tactile sensor, integrated into PRISMA hand II fingertips, present as output four voltages obtained by transducing the currents flowing into PTs in voltages, acquired through Analog-to-Digital converters available from microcontroller integrated at the base of the hand. The sensor calibration consists to identify the parameters of a model (in this paper a Neural Network) which represents the relationship between the external applied force components and the raw voltage signals available from the sensor. To this aim, voltages and force components have to be simultaneously acquired in order to prepare an adequate dataset for the calibration.

Data are collected using the suitably prepared setup (see Fig. 4), comprising of the developed fingertip sensor which is installed on a reference force sensor (ATI NANO 17 F/T Sensor) by an adapter. Then the silicone pad is pushed from various directions, using a rigid object with a flat surface. The force measurements of the reference sensor and the voltage signals of the tactile sensors are both recorded, at a sampling rate equal to 180 Hz. For each fingertip the measurements have been recorded for about 180 s, by obtaining a total of about $30,000$ data samples. The acquired data have been randomly divided into training, validation, and test subsets comprising 70%, 15%, and 15%, respectively.

Sanchez et al. [30] have used recurrent units for force estimation since their data is time-correlated. On the contrary, our data is not time-correlated. The voltage-force relationship can be treated as a time-independent feature; hence it can be represented as a mapping from voltage readings to force components for each data point. Several linear and nonlinear machine learning regression models are trained to draw the baseline. Then dense networks are trained, and the optimal one, five layers with batch normalization ($4-16-8-8-3$ neurons in layers), is selected. ReLu activations and Adam optimizer is used for training both CNN and dense networks. All the trained models have been compared by means of the Mean Absolute Error (MAE) and the Mean Squared Error (MSE) metrics. Figure 5 reports MAE and MSE computed for all trained models for the three force components reconstruction corresponding to the index finger of PRISMA hand II (the list of tested models can be evaluated from the same figure). The results obtained for other fingers are very similar. From Fig. 5 results that the best fitting can be obtained by using a fully connected neural network (FCN) and a convolutional neural network (CNN). Reshaping the vector of PT signals to construct an image allows to use a CNN, and also to take advantage of the translational invariant feature of convolutional networks. The CNN regresses the phototransistor outputs (an image composed of 2×2 pixels) to the three force components (f_x, f_y, f_z). Although the integrated sensor only have 4 PTs and hence a small image. The impact of using a CNN will be more obvious by increasing the number of PTs and the number of pixels. The network architecture is represented in Figure 6. Its training makes use of 3×3 filters with the same padding, batch normalization and dropout layers, Rectified Linear as activation function (ReLu) and Adam as optimizer. The total parameters of the network are 1675. Since both electronic components (LED-PT couples) and mechanical components (deformable layers) are custom, the characteristics of each

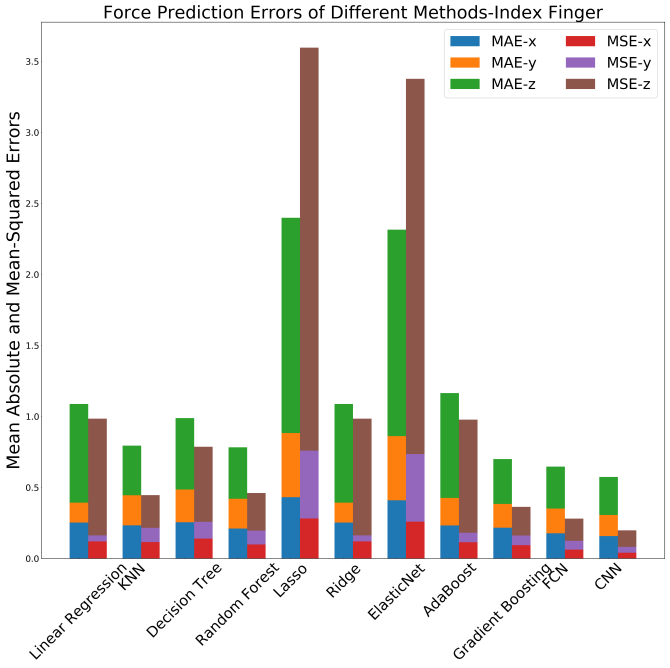

Fig. 5. Mean Absolute Error and Mean Squared Error for different models and all force components of index finger.

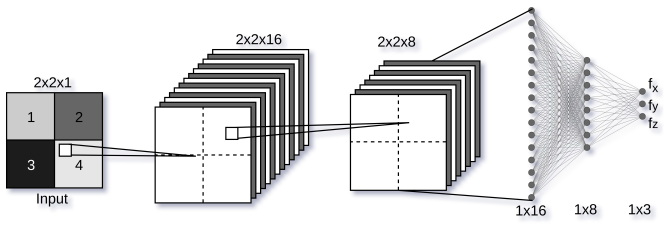

Fig. 6. Developed CNN architecture used for mapping phototransistor outputs to forces in three dimensions

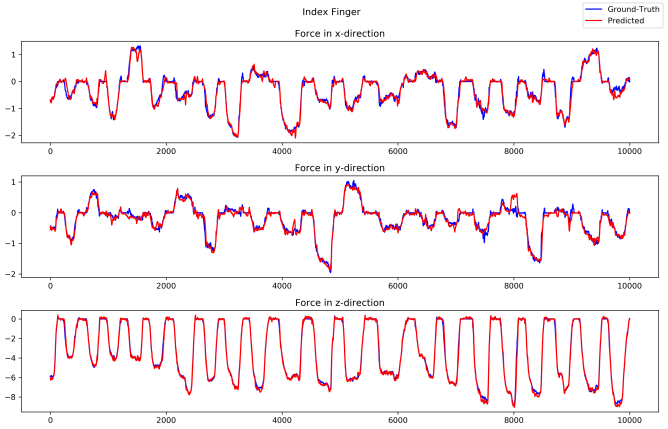

Fig. 7. Predicted and measured forces by CNN for index finger (training data).

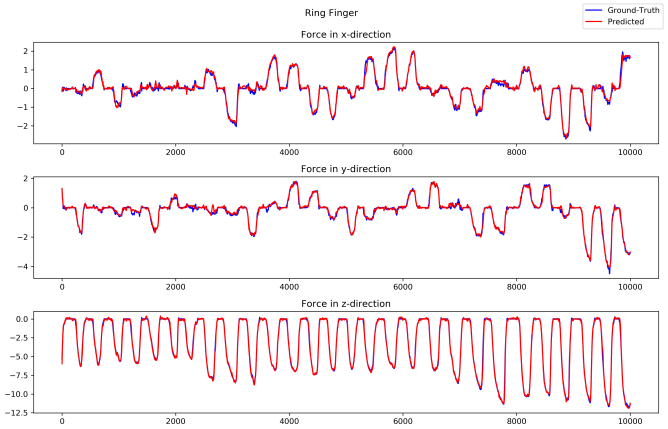

Fig. 8. Predicted and measured forces by CNN for ring finger (training data).

sensor are different for each finger, and as a consequence to obtain good results five different networks have to be trained for the five fingers. Figures 7 and 8 report the reconstruction obtained by two different networks trained for the index and the ring fingers, respectively.

V. Experiments on PRISMA hand II

In order to evaluate the effectiveness of the proposed sensing solution, some experiments with the calibrated sensors assembled on-board the PRISMA hand II have been carried out.

A. On board force estimation

The index finger of the PRISMA hand II has been used to push on the ATI NANO 17 F/T Sensor (used as ground truth for the calibration), mounted on a workbench (see Fig. 9). The objective is to compare the force reconstructed by the calibrated sensor, assembled on board the hand, and the force components measured by the ATI. For these on board tests the two best neural networks (FCN and CNN according to error values reported in Fig. 5) have been compared with the ground truth. The index finger has been pushed on the ATI sensor along the three orthogonal axes as shown in pictures reported in Fig. 9. A suitable sign compensation has been used to take into account the relative position of ATI and fingertip frames and to allow the comparison of estimated force components and the ground truth. The results in Fig. 10 show that also on board, the FCN and the CNN models present good results and similar among them. However, the CNN model is for all three components slightly better than FCN as already highlighted in the calibration phase. For both models it is evident that the normal components is reconstructed much better than tangential components. This characteristic mainly depends on deformable pad shape which well tranduces the normal external component into local deformations measured by the taxels, while the tangential components have a lower effect on taxel measurements. To increase the accuracy of the sensor, in future developments, a higher number of cells (LED-PT couples) have to be integrated on the PCB.

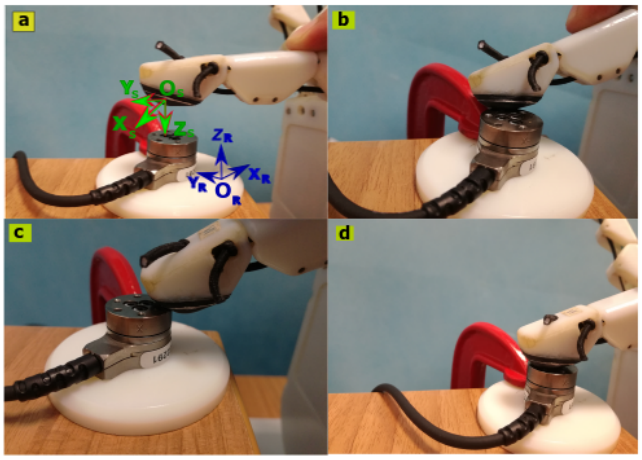

Fig. 9. On board validation of force components: reference frames of ATI and fingertip sensor (a), test along x direction (b), y direction (c) and z direction (d).

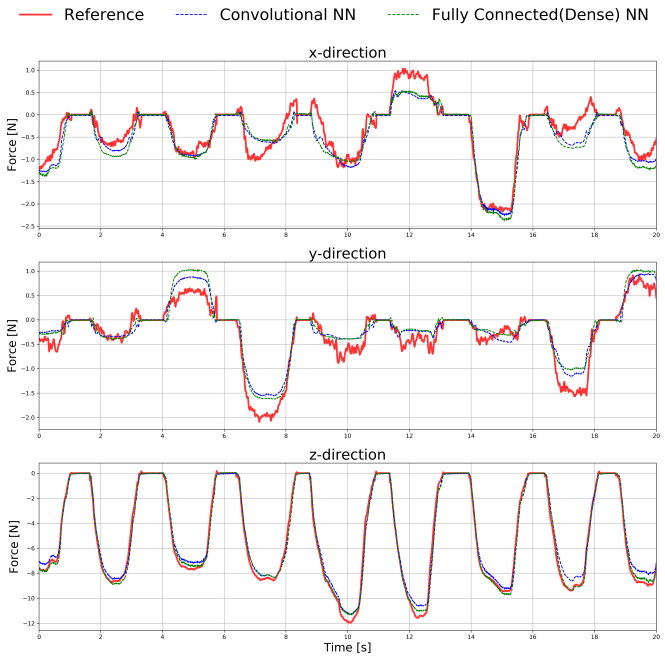

Fig. 10. Validation of estimated forces with on board assembled sensors (testing data).

B. Force adjustment

Using the CNN model for the calibration of the fingertip sensor, a force adjustment experiment has been carried out. The objective is to grasp with the PRISMA hand II a ball, by ensuring that the following no-slip condition is respected on thumb fingertip:

$$||\boldsymbol{F}_t|| \leq \mu_s \, |f_z| \tag{1}$$

where $||\boldsymbol{F}_t||$ is the norm of tangential force (combination of f_x and f_y), μ_s is the static friction coefficient and $|f_z|$ is the

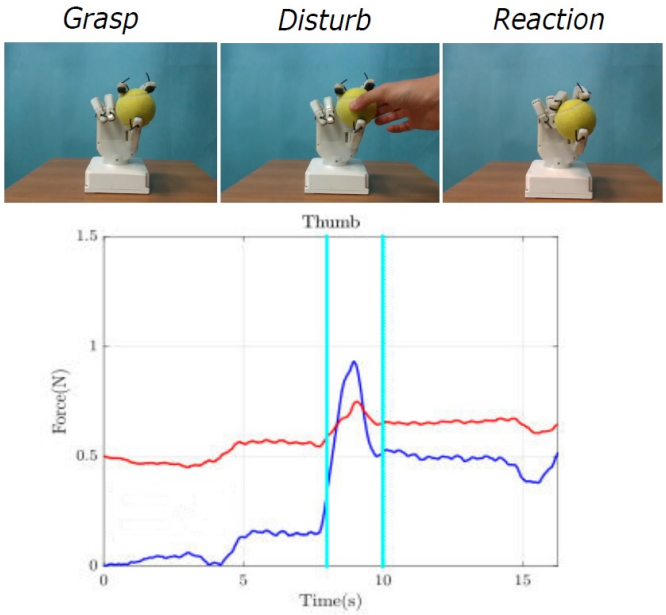

Fig. 11. Force adjustment for slipping avoidance: $||\boldsymbol{F}_t||$ blu line and $\mu_s \, |f_z|$ red line.

absolute value of normal force. In the proposed experiment, a value for $\mu_s = 0.5$ has been considered for the static friction coefficient and a tennis ball with a mass equal to $m = 0.056\,\text{Kg}$ for the grasping. The experiment consists in increase the grasp strength by acting on the finger motors proportionally, through a gain k, to the norm of tangential force estimated by the thumb, when the no-slip condition is not verified. Figure 11 reports a sequence of images and the corresponding forces estimated by the thumb for three different phases of the same experiment: at initial the tennis ball is grasped by the hand and the estimated $||\boldsymbol{F}_t||$ is well below $\mu_s \, |f_z|$ (this means that the system is away from slipping); then an operator impose a disturbance, trying to remove the ball from the hand, which corresponds to an increase of tangential force $||\boldsymbol{F}_t||$ with an increase of grasp strength according to the controller gain (in this phase, between the cyan vertical lines, the motor increase their action to avoid the slippage); finally, when the disturbance finishes the no-slip condition is restored and the control action, based on tangential force, ends.

VI. CONCLUSIONS

This paper presents a novel tactile sensing suite for the PRISMA Hand II. A brief description of the PRISMA Hand mechanical design, the tactile/force sensor technology and the data recording procedure is provided. Afterwards, a calibration technique is proposed by comparing several neural networks. In particular, some tests on datasets demonstrates that FCN and CNN are the best models to use with the proposed sensing solution. The selected models have been tested on board by exploiting the PRISMA hand II in different experiments, consisting in pushing on a reference sensor and slipping avoidance for a grasped tennis ball. Future works are needed in

order to design tactile sensors with a higher number of taxels, since the accuracy in force reconstruction is limited for the implementation of advanced manipulation tasks.

REFERENCES

[1] M. Grebenstein, M. Chalon, W. Friedl, S. Haddadin, T. Wimböck, G. Hirzinger, and R. Siegwart, "The hand of the dlr hand arm system: Designed for interaction," *The International Journal of Robotics Research*, vol. 31, no. 13, pp. 1531–1555, 2012.

[2] K. Y. Choi, A. Akhtar, and T. Bretl, "A compliant four-bar linkage mechanism that makes the fingers of a prosthetic hand more impact resistant," in *2017 IEEE International Conference on Robotics and Automation (ICRA)*. IEEE, 2017, pp. 6694–6699.

[3] J. T. Belter and A. M. Dollar, "Novel differential mechanism enabling two dof from a single actuator: Application to a prosthetic hand," in *2013 IEEE 13th International Conference on Rehabilitation Robotics (ICORR)*. IEEE, 2013, pp. 1–6.

[4] A. M. Dollar and R. D. Howe, "The highly adaptive sdm hand: Design and performance evaluation," *The international journal of robotics research*, vol. 29, no. 5, pp. 585–597, 2010.

[5] L. U. Odhner, L. P. Jentoft, M. R. Claffee, N. Corson, Y. Tenzer, R. R. Ma, M. Buehler, R. Kohout, R. D. Howe, and A. M. Dollar, "A compliant, underactuated hand for robust manipulation," *The International Journal of Robotics Research*, vol. 33, no. 5, pp. 736–752, 2014.

[6] F. Lotti, P. Tiezzi, G. Vassura, L. Biagiotti, G. Palli, and C. Melchiorri, "Development of ub hand 3: Early results," in *Proceedings of the 2005 IEEE International Conference on Robotics and Automation*. IEEE, 2005, pp. 4488–4493.

[7] M. G. Catalano, G. Grioli, E. Farnioli, A. Serio, C. Piazza, and A. Bicchi, "Adaptive synergies for the design and control of the pisa/iit softhand," *The International Journal of Robotics Research*, vol. 33, no. 5, pp. 768–782, 2014.

[8] C. Piazza, M. G. Catalano, S. B. Godfrey, M. Rossi, G. Grioli, M. Bianchi, K. Zhao, and A. Bicchi, "The softhand pro-h: a hybrid body-controlled, electrically powered hand prosthesis for daily living and working," *IEEE Robotics & Automation Magazine*, vol. 24, no. 4, pp. 87–101, 2017.

[9] G. Palli, C. Melchiorri, G. Vassura, U. Scarcia, L. Moriello, G. Berselli, A. Cavallo, G. De Maria, C. Natale, S. Pirozzi, C. May, F. Ficuciello, and B. Siciliano, "The dexmart hand: Mechatronic design and experimental evaluation of synergy-based control for human-like grasping," *International Journal of Robotics Research*, vol. 33, no. 5, pp. 799–824, 2014.

[10] F. Ficuciello, A. Federico, V. Lippiello, and B. Siciliano, "Synergies evaluation of the schunk s5fh for grasping control," *Advances in Robot Kinematics 2016*, pp. 225–233, 2018.

[11] F. Ficuciello, "Hand-arm autonomous grasping: Synergistic motions to enhance the learning process," *Intelligent Service Robotics*, Sept 2018.

[12] F. Ficuciello, D. Zaccara, and B. Siciliano, "Synergy-based policy improvement with path integrals for anthropomorphic hands," *IEEE/RSJ International Conference on Intelligent Robots and Systems*, pp. 1940–1945, 2016.

[13] I. Cerulo, F. Ficuciello, V. Lippiello, and B. Siciliano, "Teleoperation of the schunk s5fh under-actuated anthropomorphic hand using human hand motion tracking," *Robotics and Autonomous Systems*, vol. 89, pp. 75 – 84, 2017.

[14] L. Villani, V. Lippiello, F. Ruggiero, F. Ficuciello, B. Siciliano, and G. Palli, "Grasping and control of multifingered hands," in *Advanced Bimanual Manipulation*, B. Siciliano (Ed.), Springer Tracts in Advanced Robotics, vol. 80, Springer, 2012, pp. 219–266.

[15] D.-H. Lee, J.-H. Park, S.-W. Park, M.-H. Baeg, and J.-H. Bae, "Kitech-hand: A highly dexterous and modularized robotic hand," *IEEE/ASME Transactions on Mechatronics*, vol. 22, no. 2, pp. 876–887, 2016.

[16] J. Zhou, J. Yi, X. Chen, Z. Liu, and Z. Wang, "Bcl-13: A 13-dof soft robotic hand for dexterous grasping and in-hand manipulation," *IEEE Robotics and Automation Letters*, vol. 3, no. 4, pp. 3379–3386, 2018.

[17] K. Xu, H. Liu, Z. Liu, Y. Du, and X. Zhu, "A single-actuator prosthetic hand using a continuum differential mechanism," in *2015 IEEE International Conference on Robotics and Automation (ICRA)*. IEEE, 2015, pp. 6457–6462.

[18] F. Ficuciello, "Synergy-based control of underactuated anthropomorphic hands," *IEEE Transactions on Industrial Informatics*, vol. 15, no. 2, pp. 1144–1152, Feb 2019.

[19] F. Ficuciello, G. Palli, C. Melchiorri, and B. Siciliano, *Postural Synergies and Neural Network for Autonomous Grasping: a Tool for Dextrous Prosthetic and Robotic Hands*. Springer Berlin Heidelberg, 2012, ch. Converging Clinical and Engineering Research on Neurorehabilitation, Biosystems and Biorobotics, pp. 467–480.

[20] L. U. Odhner and A. M. Dollar, "Stable, open-loop precision manipulation with underactuated hands," *The International Journal of Robotics Research*, vol. 34, no. 11, pp. 1347–1360, 2015.

[21] N. Rojas, R. R. Ma, and A. M. Dollar, "The gr2 gripper: an underactuated hand for open-loop in-hand planar manipulation," *IEEE Transactions on Robotics*, vol. 32, no. 3, pp. 763–770, 2016.

[22] B. Ward-Cherrier, N. Rojas, and N. F. Lepora, "Model-free precise in-hand manipulation with a 3d-printed tactile gripper," *IEEE Robotics and Automation Letters*, vol. 2, no. 4, pp. 2056–2063, 2017.

[23] R. R. Ma, W. G. Bircher, and A. M. Dollar, "Toward robust, whole-hand caging manipulation with underactuated hands," in *2017 IEEE International Conference on Robotics and Automation (ICRA)*. IEEE, 2017, pp. 1336–1342.

[24] C. Della Santina, C. Piazza, G. Grioli, M. G. Catalano, and A. Bicchi, "Toward dexterous manipulation with augmented adaptive synergies: The pisa/iit softhand 2," *IEEE Transactions on Robotics*, vol. 34, no. 5, pp. 1141–1156, 2018.

[25] H. Yousef, M. Boukallel, and K. Althoefer, "Tactile sensing for dexterous in-hand manipulation in robotics—a review," *Sensors and Actuators A: physical*, vol. 167, no. 2, pp. 171–187, 2011.

[26] G. De Maria, C. Natale, and S. Pirozzi, "Force/tactile sensor for robotic applications," *Sensors and Actuators A: Physical*, vol. 175, pp. 60–72, 2012.

[27] A. D'Amore, G. De Maria, L. Grassia, C. Natale, and S. Pirozzi, "Silicone-rubber-based tactile sensors for the measurement of normal and tangential components of the contact force," *Journal of Applied Polymer Science*, vol. 122, no. 6, pp. 3757–3769, 2011.

[28] H. Liu, P. Ferrentino, S. Pirozzi, B. Siciliano, and F. Ficuciello, "The PRISMA Hand ii: A Sensorized Robust Hand for Adaptive Grasp and In-Hand Manipulation," in *2019 International Symposium on Robotics Research (ISRR)*, 2019.

[29] J. R. Cannon, C. P. Lusk, and L. L. Howell, "Compliant rolling-contact element mechanisms," in *ASME 2005 international design engineering technical conferences and computers and information in engineering conference*. American Society of Mechanical Engineers Digital Collection, 2008, pp. 3–13.

[30] J. Sanchez, C. M. Mateo, J. A. Corrales, B. C. Bouzgarrou, and Y. Mezouar, "Online shape estimation based on tactile sensing and deformation modeling for robot manipulation," in *2018 IEEE/RSJ International Conference on Intelligent Robots and Systems (IROS)*, 2018, pp. 504–511.